Influence of the Metal Ion on the Two-Photon Absorption Properties of Lanthanide Complexes Including Near-IR Emitters

9 AUTHORS, INCLUDING:

Mustapha Allali

High Institute of health careers Fes/ ISPITS-…

16 PUBLICATIONS **150** CITATIONS

SEE PROFILE

Anthony D'Aléo

CINaM - Centre Interdisciplinaire de Nanosc…

53 PUBLICATIONS **792** CITATIONS

SEE PROFILE

Chantal Andraud

Claude Bernard University Lyon 1

221 PUBLICATIONS **2,937** CITATIONS

SEE PROFILE

Olivier Maury

Ecole normale supérieure de Lyon

169 PUBLICATIONS **3,344** CITATIONS

SEE PROFILE

Influence of the Metal Ion on the Two-Photon Absorption Properties of Lanthanide Complexes Including Near-IR Emitters

Adrien Bourdolle,[a] Mustapha Allali,[a] Anthony D'Aléo,[a] Patrice L. Baldeck,[a] Kenji Kamada,[b] J. A. Gareth Williams,[c] Hubert Le Bozec,[d] Chantal Andraud,*[a] and Olivier Maury*[a]

The synthesis of tris(2-thenoyltrifluoroacetonate)lanthanide(III) complexes featuring a diethylaminostyryl-2,2′-bipyridine coligand was achieved for lanthanum; the near-infrared (NIR) emitters neodymium, erbium, and ytterbium; and the transition-metal yttrium. The photophysical properties were thoroughly studied, and it was demonstrated that the conjugated bipyridine ligand acts as a good antenna for the sensitization of the NIR emitters. The two-photon absorption (TPA) properties of all five complexes were investigated by using both two-photon excited fluorescence and the Z-scan method. We demonstrate that the nature of the rare earth ion has almost no influence on the TPA properties centered on the conjugated bipyridyl ligand. Finally, we show that Yb[III] is sensitized by a two-photon antenna effect, and that Nd[III] is mostly sensitized by a one-photon process involving direct excitation of forbidden f–f transitions.

1. Introduction

In the last decade, the study of the two-photon absorption (TPA) properties of lanthanide complexes[1] has been a challenging research area with the objective to combine the unique photophysical properties of f elements[2] [sharp emission bands with large pseudo-Stokes shifts ranging from the visible region to the near-infrared (NIR) region and long lifetimes enabling time-delayed detection] with the intrinsic advantage of TPA excitation[3] (NIR excitation with confocal character, which gives rise to 3D resolution). Such complexes should present high potential as bioprobes for biphotonic bioimaging applications. Following the seminal report of Lakowicz[4] and proof-of-concept of the two-photon antenna effect,[5] numerous examples of two-photon microscopy imaging of cells by using either terbium[6] or europium[7] complexes have been reported. Recently, the two-photon sensitization of ytterbium emitting in the NIR spectral range was achieved, and the two-photon cross sections of the complexes were optimized.[8] The NIR emission of ytterbium opens up exciting perspectives for thick-tissue imaging, and in this context, we recently reported the blood vascular network imaging of a mouse brain slice by using a homemade two-photon microscopy apparatus working in an unconventional NIR-to-NIR configuration.[9]

In this article, we report our first attempt to generalize two-photon sensitization to other NIR emitters, namely, neodymium and erbium. To that end, model complexes of the type Ln(TTA)$_3$DEASbpy (TTA = 2-thenoyltrifluoroacetonate) featuring an additional diethylaminostyryl-2,2′-bipyridine (DEASbpy) ligand were prepared with various rare earth ions (Ln = La, Nd, Er, Yb, and Y). The DEASbpy ligand was chosen because of its well-known ability to generate stable transition-metal complexes exhibiting large second-[10] or third-order[11] nonlinear optical (NLO) properties. The photophysical properties of the complexes were carefully studied, and the DEASbpy ligand appeared to be a good antenna for the sensitization of the NIR emitters. Finally, the TPA cross section (σ^2) of these complexes was determined by using both two-photon excited fluorescence (TPEF) and the Z-scan method. The influence of the metal center on the NLO properties is also discussed, and the behavior of neodymium and erbium is underlined. Notably, we show that the unique photophysical properties of lanthanide ions, which are generally considered as a great advantage for two-photon microscopy, can sometimes present some drawbacks that severely limit or even prohibit their use for this application.

[a] Dr. A. Bourdolle, Dr. M. Allali, Dr. A. D'Aléo, Dr. P. L. Baldeck, Dr. C. Andraud, Dr. O. Maury
University Lyon 1, ENS Lyon, CNRS UMR 5182
46 allée d'Italie 69364 Lyon (France)
E-mail: chantal.andraud@ens-lyon.fr
        olivier.maury@ens-lyon.fr

[b] Dr. K. Kamada
Research Institute for Ubiquitous Energy Devices
National Institute of Advanced Industrial Science and Technology (AIST)
AIST Kansai Center, 1-8-31 Midorigaoka, Ikeda
Osaka 563-8577 (Japan)

[c] Prof. J. A. G. Williams
Department of Chemistry
Durham University, South Road, Durham, DH1 3 LE (UK)

[d] Dr. H. Le Bozec
Université de Rennes 1, Sciences Chimiques de Rennes
UMR 6226 CNRS, Campus de Beaulieu
35042 Rennes Cedex (France)

2. Results and Discussion

Synthesis

The preparation of the Ln(TTA)$_3$DEASbpy complexes was achieved in a one-pot, two-step procedure already described for other bis(imine) ligands.[12] Typically, a dichloromethane solution of DEASbpy and an ethanol solution of the lanthanide chloride salt were added to a solution of thenoyltrifluoroacetone (3 equiv.) deprotonated with sodium hydroxide in ethanol (Scheme 1). All of the Ln(TTA)$_3$DEASbpy (Ln = Y, La, Nd, Yb, Er) complexes were isolated in good yield and all were fully char-
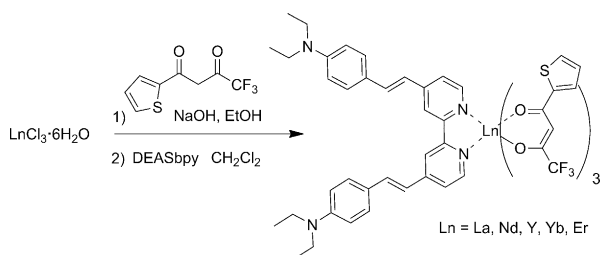
Scheme 1. Synthesis of the target complexes.

acterized by ^{1}H NMR, ^{19}F NMR, and FTIR spectroscopy. Elemental analysis clearly confirmed the stoichiometry of the complexes (see the Experimental Section for details). In the NMR spectra, only one set of signals is observed at room temperature, and this is in agreement with a threefold solution structure of the TTA ligands around the metal center.[13] The DEASbpy ligand also displays one set of signals spread over 40 ppm due to the paramagnetic lanthanide ions. Notably, in all cases the *trans* configuration of the double bond is retained, as shown by the large $^3J_{H,H}$ coupling constant of approximately 16 Hz.

Photophysical Characterization

The study of the absorption and emission properties was performed in dilute dichloromethane solution at room temperature, and the results are compiled in Table 1. As already observed, the DEASbpy ligand presents broad, intense absorption and emission bands assigned to an intramolecular charge-transfer (CT) transition from the diethylamino donor to the pyridine acceptor moieties.[10,11] As illustrated in Figure 1, in the case of the yttrium complex, the coordination of DEASbpy to the Ln(TTA)$_3$ fragment increases the electron-withdrawing character of the bipyridine unit, which results in a strong bathochromic shift of
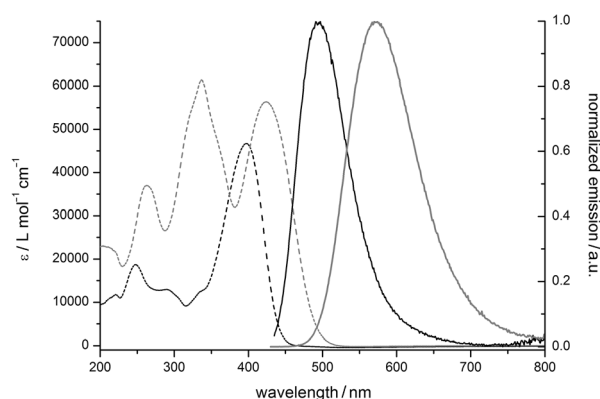

Figure 1. UV/Vis electronic absorption spectra (-----) and emission spectra (——) of the DEASbpy ligand and the absorption spectra (-----) and emission spectra (——) of Y(TTA)$_3$DEASbpy in dichloromethane solution at room temperature.

the absorption ($\Delta\lambda = 25$ nm) and emission ($\Delta\lambda = 60$–90 nm) bands. The wavelength of the maximum absorption does not depend on the identity of the central lanthanide ion (Table 1), which is in agreement with previous literature results.[14] In contrast, the evolution of the maximum emission wavelength, λ^{CT} assigned to CT emission, follows the decreasing radii of the Ln^{3+} ions along the series, that is, lanthanide contraction (La > Nd > Y > Er > Yb), and, hence, the increase in Lewis acidity. Upon coordination to Y(TTA)$_3$, the emission quantum yield is more than fourfold enhanced relative to that of the free ligand, from 0.11 to 0.48 (Table 1). This phenomenon has already been observed in the case of related zinc(II) complexes and is explained by the stiffening of the bipyridine ligand due to its coordination to the metal ion, that is, the rotation around the 2,2′ bond is blocked, which limits nonradiative de-excitation pathways.[11c] In contrast to Y^{III}, coordination to Yb^{III}, Nd^{III}, and Er^{III} results in significant quenching of the ligand-centered emission, and the corresponding fluorescence quantum yields are 0.02, 0.08, and 0.01 respectively (Table 1). This quenching is the signature of efficient energy transfer to the lanthanide excited state, which induces their characteristic NIR emission (λ^{Ln}) at 979 (Yb^{III} $^2F_{5/2} \rightarrow {}^2F_{7/2}$); 897, 1062, and 1336 (Nd^{III} $^4F_{3/2} \rightarrow {}^4I_{9/2}$, $^4F_{3/2} \rightarrow {}^4I_{11/2}$, and $^4F_{3/2} \rightarrow {}^4I_{13/2}$, respectively), and 1531 nm (Er^{III} $^4I_{13/2} \rightarrow {}^4I_{15/2}$) (Figure 2). The efficiency of the trans-

Table 1. Linear and nonlinear photophysical data of DEASbpy and related complexes in dichloromethane solution.

	Absorption λ [nm] (ε [L mol^{-1} cm^{-1}])	Emission λ^{CT} [nm] (Φ)[a]	λ^{Ln} nm (τ [µs])	TPA[b] λ^2 nm (σ^2 [GM])
DEASbpy	399 (64 000)	496 (0.11)	–	770 (225)
Y(TTA)$_3$DEASbpy	423 (65 000)	567 (0.48)	–	850 (237) 850 (232)[c]
La(TTA)$_3$DEASbpy	422 (52 000)	542	–	850 (184)[c]
Nd(TTA)$_3$DEASbpy	423 (64 000)	556 (0.08)	1062 (0.98)	840 (220)
Er(TTA)$_3$DEASbpy	423 (64 000)	571 (0.01)	1531 (1.66)	840 (110)
Yb(TTA)$_3$DEASbpy	424 (59 000)	584 (0.02)	979 (9.38)	830 (230) 850 (214)[c]

[a] Coumarin-153 in MeOH was used as a standard ($\Phi = 0.45$). [b] Measured by TPEF by using the ICT emission band. [c] Value in parentheses was measured by the Z-scan method.
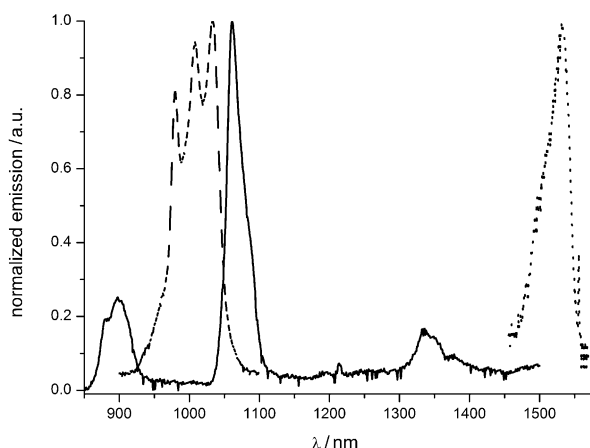
Figure 2. NIR emission of the Ln(TTA)$_3$DEASbpy complexes in dichloromethane solution at room temperature. Ln = Yb (– – –), Nd (——), and Er (•••••).

fer is illustrated by the magnitude of quenching, and thus, DEASbpy sensitization efficiency follows the series Er > Yb > Nd. The charge-transfer (CT) nature of the absorption band suggests a direct sensitization pathway from the ligand CT excited state now frequently invoked in the literature.[15] The Ln-centered emission lifetimes (Table 1) are typical for such structures.[16]

TPA Properties

The TPA properties were determined by TPEF and/or by the Z-scan method (Table 1). The TPEF measurements, which consist of determining the two-photon brightness $\sigma^2\Phi$ (see the Experimental Section), were conducted by using only the (residual) CT emission centered on the ligand. The NIR emission could not be considered for quantitative determination due to the low sensitivity of our detector in this spectral range. The TPA spectra of Y(TTA)$_3$DEASbpy measured by the two methods are compared in Figure 3, and it is clear that there is very good agreement between the two methods: the maximum TPA
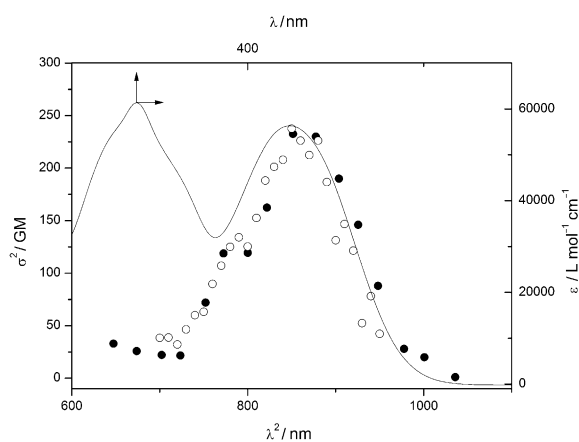

Figure 3. TPA spectra of Y(TTA)$_3$DEASbpy in CH$_2$Cl$_2$ measured by TPEF (○) and Z-scan (●). Superimposed on this plot is the single photon absorption (——, upper abscissa).

wavelengths (λ^2) are identical and the maximum two-photon cross sections (σ^2) match very well (237 vs 232 nm for TPEF and Z-scan, respectively) considering the relative experimental error of ±20% in the NLO measurements. Notably, the TPA spectrum can almost be exactly superimposed onto the wavelength-doubled one-photon absorption spectrum, and this is in agreement with the two-photon section rules for noncentrosymmetric chromophores.[3] This result indicates that the excited state from which energy transfer occurs, and consequently the lanthanide sensitization pathway, is the same for both one- and two-photon excitation.[5c]

The TPA spectra of Ln(TTA)$_3$DEASbpy (Ln = Y, Nd, Yb, Er) measured by the TPEF method are compared in Figure 4. In all
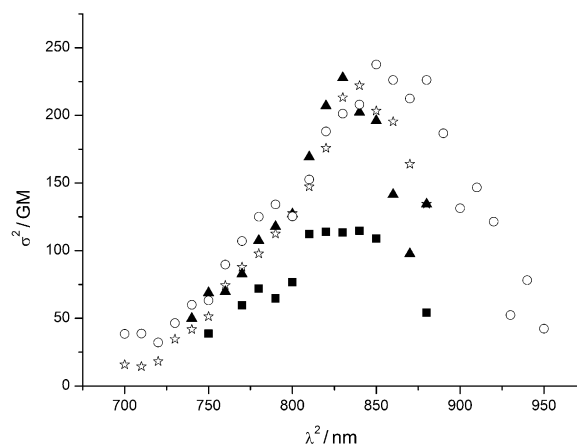
Figure 4. TPA spectra in CH$_2$Cl$_2$ measured by TPEF in the ligand-centered CT emission of Ln(TTA)$_3$DEASbpy Ln = Y (○), Yb (▲), Nd (☆), Er (■).

cases, the ligand-centered CT emission exhibits an almost perfectly quadratic dependence on the incident laser power P, as illustrated by the slope a^{CT} of 1.88, 1.96, 1.86, and 1.91 (Figure 6). The TPA profiles of the Y^{III}, Yb^{III}, and Nd^{III} complexes are very similar, and the apparent differences are within experimental error. The TPA spectrum of the Er complex shows a σ^2 value of 105 GM, which corresponds to about half of that of the other complexes. At this stage, one must remember that TPEF measurements involve the determination of the two-photon brightness $\sigma^2\Phi$, and that in the case of Er-(TTA)$_3$DEASbpy, the residual CT transition exhibits a very low fluorescence quantum yield of 0.01. Consequently, the experimental error of the σ^2 value is very high due to the uncertainty in the determination of such a low fluorescence quantum yield combined with the inherent uncertainty in the TPEF measurement. Therefore, on the basis of these measurements only, it is impossible to draw any definitive conclusions about the influence of the central metal ion on the TPA properties. To tackle the drawback of the quantum yield determination, TPA measurements were also performed by using open-aperture Z-scan experiments for the Y^{III}, La^{III}, and Yb^{III} complexes (Figure 5). By this technique, the uncertainty of the experimental data is much lower and, more importantly, similar for each complex. It appears that the TPA spectra are exactly the same, regardless
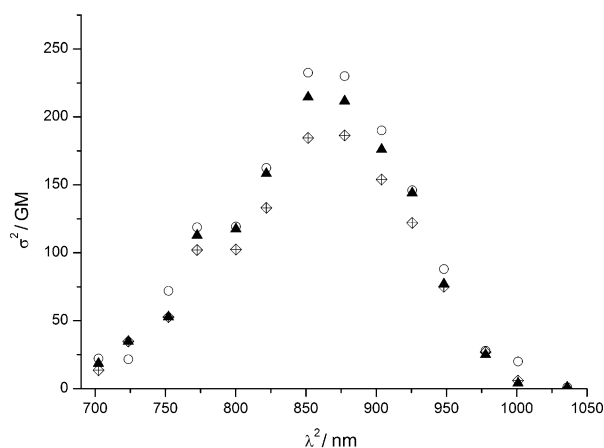
Figure 5. TPA spectra in CH_2Cl_2 measured by Z-scan of Ln(TTA)$_3$DEASbpy Ln = Y (○), Yb (▲), La (◇).

of the nature of the central metal ion (ionic radius or f orbital filling). In marked contrast to the second-order NLO properties of lanthanide complexes,[17] the TPA properties, which are related to the imaginary part of the third-order hyperpolarizability (third-order NLO properties), seem to be controlled only by the nature of the ligand and are independent of the nature of the central f-block element.

As noted above, one of the major characteristics of the TPA process is the quadratic dependence of the emission intensity on the incident laser power, a property responsible for the 3D spatial resolution of TPA-based applications. We also checked this variation for the NIR emission of the Ln(TTA)$_3$DEASbpy complexes (Ln = Yb, Nd, Er). Using our experimental setup, only the highest-energy Ln-centered transition for Yb and Nd could be monitored (Figure 6); in the case of erbium, the $^4F_{13/2}$ → $^4I_{15/2}$ transition is located out of the detection range, and consequently, it was impossible to measure its variation. As with all residual CT emission, Yb^{III} emission shows quadratic variation with the incident laser power (a^{Yb} = 2.09), which thus

confirms unambiguously the CT-mediated two-photon sensitization pathway. In marked contrast, neodymium emission presents almost linear variation with the incident laser power (a^{Nd} = 1.13), which is indicative of a preponderant one-photon photophysical process. This result can be explained by the fact that the neodymium ion possess two absorption bands of low intensity around 730 and 800 nm ($\varepsilon < 0.1$ L mol^{-1} cm^{-1}, see Figure 7 for NdCl$_3$ in water) assigned to the parity-forbidden
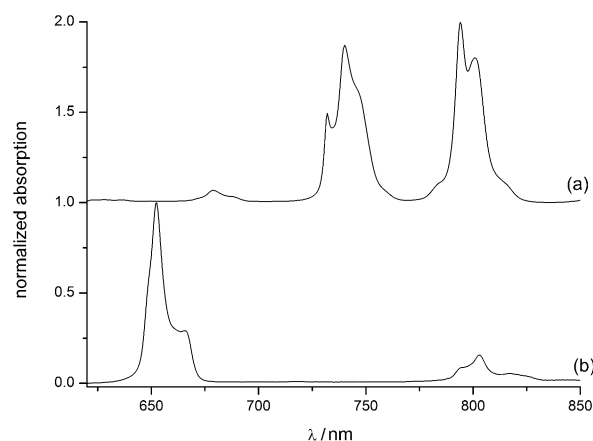
Figure 7. The electronic absorption spectra in the 600–850 nm range of concentrated solutions of LnCl$_3$ in water for a) Ln = Nd and b) Ln = Er.

$^4I_{9/2}$ → $^2H_{9/2}$ transition and to the symmetry-forbidden $^4I_{9/2}$ → $^4S_{3/2}$ transition, respectively.[18] The linear relationship between emission and laser power unambiguously indicates that neodymium emission mainly arises from linear absorption in the forbidden f–f transitions and that the two-photon antenna effect is completely masked by this linear phenomenon. Indeed, it is interesting to note that at the same time, the two-photon excitation occurs to yield the two-photon-induced fluorescence of the CT state. Similar behavior was already reported for the excitation of a europium tris(dipicolinate) complex at 532 nm.[6a] This result indicates that neodymium complexes are not suitable for TPA-based applications with the use of a Ti:sapphire laser source.

3. Conclusions

Ln(TTA)$_3$DEAbpy complexes (Ln = La, Y, Nd, Er, Yb) featuring a conjugated bipyridine ligand present similar TPA behavior irrespective of the identity of the central f-block ion. This result is in marked contrast to second-order NLO activity, in which the identity of the lanthanide plays a pivotal role.[10, 11] Whereas Yb^{III} luminescence can be sensitized by a two-photon antenna process in the 700–900 nm spectral range corresponding to the Ti:sapphire source, the presence of forbidden f–f absorptions restricts the two-photon excitation range around 700–750 nm for erbium and completely prohibits two-photon sensitization in the case of neodymium, which precludes the use of this element for any TPA-based applications in the 700–900 nm range.
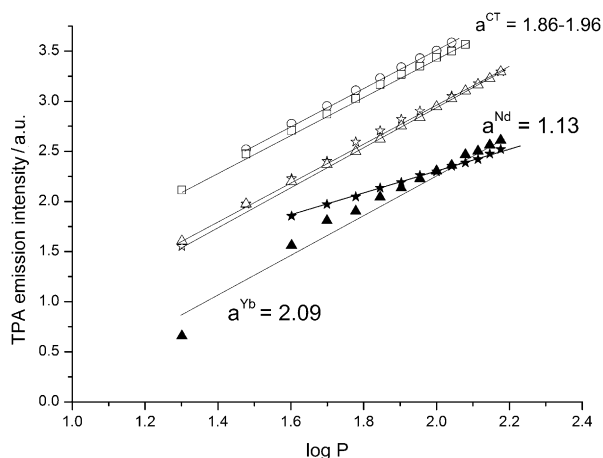

Figure 6. Variation of the luminescence intensity versus the incident laser power in log scale for the residual CT emission (open symbol) and for the metal-centered emission (black symbol) of LLn(TTA)$_3$ complexes: Ln = Y (○), Yb (△/▲), Nd (open star ☆/★), Er (□).

Experimental Section

General Procedure

NMR spectra (^{1}H, ^{13}C) were recorded at room temperature with a Bruker AC 200 instrument operating at 200.13 and 50.32 MHz for ^{1}H and ^{13}C, respectively, or a Bruker Advance instrument operating at 500.10 and 125.75 MHz for ^{1}H and ^{13}C, respectively. Data are listed in parts per million (ppm) and are reported relative to tetramethylsilane (^{1}H, ^{13}C); residual solvent peaks of the deuterated solvents were used as internal standard. UV/Vis absorption measurements were recorded with a Jasco V670 absorption spectrometer. The DEAbpy ligand was prepared according to the literature.[19]

Luminescence

Emission spectra were measured by using a Horiba-Jobin Yvon Fluorolog-3 spectrofluorimeter equipped with three-slit double-grating excitation and emission monochromators with dispersions of 2.1 nm mm^{-1} (1200 grooves mm^{-1}). The steady-state luminescence was excited by unpolarized light from a 450 W xenon CW lamp and detected at an angle of 90° for diluted solution measurements (10 mm quartz cell) with a red-sensitive Hamamatsu R928 photomultiplier tube. Spectra were reference corrected for variations in the excitation source light intensity (lamp and grating) and for the emission spectral response (detector and grating). Luminescence quantum yields Q were measured in diluted dichloromethane solution with an absorbance lower than 0.1 by using Equation (1):

$$Q_x/Q_r = [A_r(\lambda)/A_x(\lambda)][n_x^2/n_r^2][D_x/D_r] \tag{1}$$

in which A is the absorbance at the excitation wavelength (λ), n is the refractive index, and D is the integrated luminescence intensity; the indexes "r" and "x" refer to the reference and the sample, respectively. The reference was Coumarin-153 in methanol (Q_r = 0.45). Excitation of the reference and the sample compounds was performed at the same wavelength. Luminescence lifetimes in the NIR region were recorded by following pulsed excitation at 337 nm with a nitrogen laser operating at 10 Hz. Emitted light detected at right angles was passed through an NIR-optimized grating and detected by using a Hamamatsu H10330 NIR photomultiplier tube operating in photon-counting mode. Exponential fitting of the data was performed by using standard nonlinear least-squares methods.

TPEF Measurements

The TPA spectra were measured according to the method of Xu and Webb.[20] The TPA cross section spectrum was obtained by upconversion luminescence by using a Ti:sapphire femtosecond laser in the 700–900 nm range. The excitation beam (5 mm diameter) was focalized with a lens (focal length 10 cm) at the middle of the 10 mm cell. Emitted light was collected at 90° and was focused into an optical fiber (diameter 600 μm) connected to an Ocean Optics S2000 spectrometer. The incident beam intensity was adjusted to 50 mW to ensure an intensity-squared dependence of the luminescence over the whole spectral range. The detector integration time was fixed to 1 s. Calibration of the spectra was performed by comparison with the published 700–900 nm Coumarin-307 TPA spectrum (quantum yield = 0.56 in ethanol). The measurements were done at room temperature in dichloromethane and at a concentration of 10^{-4} M by using Equation (2):

$$\sigma^2_s = \sigma^2_r x (S_s n_r \Phi_r C_r)/(S_r n_s \Phi_s C_s) \tag{2}$$

in which S is the area of the fluorescence spectra, n is the refractive index, Φ is the quantum yield, C is the concentration, and σ^2 is the two-photon cross section; the indexes "s" and "r" refer to the substrate and the reference, respectively.

Two-Photon Z-Scan Measurements

As another method for TPA spectra measurement based on a different principle, the open-aperture Z-scan technique was employed.[21] The details of our setup for this method was reported previously.[22] A femtosecond optical parametric amplifier pumped by a Ti:sapphire regenerative amplifier (typical pulsewidth ≈ 120 fs) was used to scan the excitation wavelength for 650–1050 nm. The sample position was scanned at several different incident powers from 0.05 to 0.4 mW (repetition rate of 1 kHz), which corresponds to an on-axis peak intensity of 20–200 GW cm^{-2} at the focal position, for each sample. The obtained Z-scan traces at the different powers were analyzed by the global curve-fitting procedure with the theoretical model by assuming a TPA process for the temporally and spatially Gaussian pulses.[22] Reasonable curve fits were obtained, which indicates that TPA is the dominant process for all data. The sample compounds were dissolved in dichloromethane with a concentration of 0.3–0.43 mM and held in a 2 mm quartz cuvette for the measurements. This optical path length of the sample was shorter than the Rayleigh range of the optics (4–5 mm), which fulfills the thin-sample condition to justify the analysis. The in-house standard compound[23] was always measured under the same conditions as those used for the samples and those used to calibrate the σ^2 values calculated from the TPA coefficients of the sample solutions obtained by the curve-fitting analysis.

General Procedure for the Preparation of the Complexes

H(TTA) (1.62 mmol, 3 equiv.) was added to a solution of NaOH (1.62 mmol, 3 equiv.) in EtOH (10 mL). The mixture was stirred for 15 min at 50°C, and then a solution of DEASbpy (0.54 mmol, 1 equiv.) in dichloromethane (10 mL) was added to afford a yellow shady solution. This mixture was then added to a solution of LnX$_3$·6H$_2$O (0.54 mmol, 1 equiv.) in EtOH (10 mL; Ln = Y, Nd, Er, Yb; X = Cl, NO$_3$). The resulting red solution was stirred under an atmosphere of nitrogen at 60°C for 3 h and then at room temperature overnight. The red solution was extracted with dichloromethane (40 mL) and washed twice with H$_2$O (50 mL). The resulting organic phase was dried with sodium sulfate, and the solvents were removed to afford a red solid. This red solid was solubilized in dichloromethane, precipitated in pentane, filtered, and then dried under vacuum.

Characterization

Y(TTA)$_3$DEASbpy: ^{1}H NMR (200.13 MHz, CDCl$_3$): δ = 9.21 (d, J = 6.0 Hz, 2H, H-6), 7.92 (s, 2H, H-3), 7.57 (q, J = 3.8 Hz, 3H, H-t$_3$), 7.47 (d, J = 4.4 Hz, 3H, H-t$_1$), 7.43 (s, 2H, H-5), 7.40 (d, J = 8.8 Hz, 4H, H-10), 7.34 (d, J = 16.2 Hz, 2H, H-8), 7.00 (dd, J = 4.4, 3.8 Hz, 3H, H-t$_3$), 6.84 (d, J = 16.2 Hz, 2H, H-8), 6.66 (d, J = 8.8 Hz, 4H, H-11), 3.39 (q, J = 7.0 Hz, 8H, H-14), 1.19 ppm (t, J = 7.0 Hz, 12H, H-15). ^{13}C NMR (125.76 MHz, CDCl$_3$): δ = 181.2 (C-b, C-d), 171.1 (C-a), 153.8 (C-2), 151.1 (C-6), 148.8 (C-e), 148.6 (C-4), 145.9 (C-12), 135.6 (C-8), 132.2 (C-t$_1$), 129.7 (C-t$_3$), 129.2 (C-10), 128 (C-t$_2$), 122.9 (C-9), 120.5 (C-5), 119.6 (C-7), 117.4 (C-3), 111.6 (C-11), 92.1 (C-c), 44.6 (C-14), 12.8 ppm (C-15). ^{19}F NMR (188.29 MHz, CDCl$_3$): δ = −75.59 ppm. IR (KBr): $\tilde{\nu}$ = 1606, 1589 cm^{-1} (vs. $\nu_{C=O}$). Elemental analysis calcd (%)
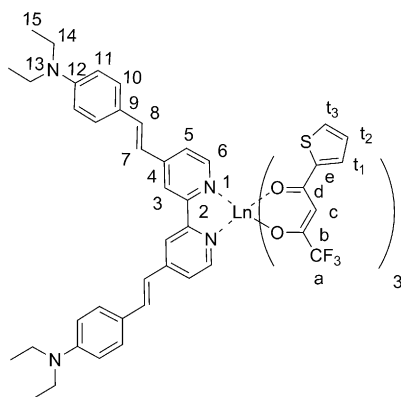
for $C_{58}H_{50}F_9N_4O_6S_3Y$: C 55.50, H 4.02, N 4.46; found: C 55.01, H 4.02, N 4.46.

La(TTA)$_3$DEASbpy: ^{1}H NMR (200.13 MHz, CDCl$_3$): $\delta = 9.09$ (d, $J = 6.0$ Hz, 2H, H-6), 7.89 (s, 2H, H-3), 7.56 (q, $J = 3.8$ Hz, 3H, H-t$_3$), 7.46 (d, $J = 4.4$ Hz, 3H, H-t$_1$), 7.41 (s, 2H, H-5), 7.39 (d, $J = 8.8$ Hz, 4H, H-10), 7.32 (d, $J = 16.2$ Hz, 2H, H-8), 6.99 (dd, $J = 4.4$, 3.8 Hz, 3H, H-t$_3$), 6.84 (d, $J = 16.2$ Hz, 2H, H-8), 6.67 (d, $J = 8.8$ Hz, 4H, H-11), 3.39 (q, $J = 7.0$ Hz, 8H, H-14), 1.19 ppm (t, $J = 7.0$ Hz, 12H, H-15). IR (KBr): $\tilde{\nu} = 1606$, 1589 cm^{-1} (vs. $\nu_{C=O}$). Elemental analysis calcd (%) for $C_{58}H_{50}F_9LaN_4O_6S_3$·CH$_2Cl_2$: C 50.98, H 3.77, N 4.03; found: C 50.24, H 3.52, N 3.74

For the other paramagnetic lanthanide complexes, it was not possible to assign all of the signals precisely. On the basis of the integral, it was possible to differentiate H-T = H-t$_1$, H-t$_2$, and H-t$_3$ from H-B = H-6, H-5, and H-3 and from the remaining protons H-c, H-7, H-8, H-10, H-11, H-14, and H-15.

Nd(TTA)$_3$DEASbpy: ^{1}H NMR (200.13 MHz, CDCl$_3$): $\delta = 10.50$ (s, 3H, H-T), 8.80 (s, 3H, H-T), 7.80 (s, 3H, H-T), 7.38 (s, 2H, H-B), 7.06 (d, $J = 7.8$ Hz, 4H, H-10), 6.67 (d, $J = 15.6$ Hz, 2H, H-8), 6.50 (s, 2H, H-B), 6.45 (d, $J = 7.8$ Hz, 4H, H-11), 5.94 (s, 2H, H-B), 5.66 (d, $J = 15.6$ Hz, 2H, H-7), 3.27 (m, 8H, H-14), 1.45 (s, 3H, H-c), 1.08 ppm (m, 12H, H-15). ^{19}F NMR (188.29 MHz, CDCl$_3$): $\delta = -75.73$ ppm. IR (KBr): $\tilde{\nu} = 1604$, 1589 cm^{-1} (vs. $\nu_{C=O}$). Elemental analysis calcd (%) for $C_{58}H_{50}F_9N_4NdO_6S_3$: C 53.16, H 3.85, N 4.28; found: C 52.59, H 3.85, N 4.28.

Er(TTA)$_3$DEASbpy: ^{1}H NMR (200.13 MHz, CDCl$_3$): $\delta = 20.14$ (s, 2H, H-B), 16.90 (s, 2H, H-B), 12.77 (s, 2H, H-8), 12.02 (s, 2H, H-7), 9.70 (d, $J = 6.8$ Hz, 4H, H-10), 7.86 (d, $J = 6.8$ Hz, 4H, H-11), 7.62 (s, 3H, H-T), 5.90 (s, 3H, H-T), 4.10 (m, 8H, H-14), 3.58 (s, 2H, H-B), 1.80 (m, 12H, H-15), 1.69 (s, 3H, H-T), -13.73 ppm (s, 3H, H-c). IR (KBr): $\tilde{\nu} = 1604$, 1587 cm^{-1} (vs. $\nu_{C=O}$). ^{19}F NMR (188.29 MHz, CDCl$_3$): $\delta = -91.57$ ppm. Elemental analysis calcd (%) for $C_{58}ErH_{50}F_9N_4O_6S_3$: C 52.24, H 3.78, N 4.20; found: C 51.84, H 3.72, N 4.20.

Yb(TTA)$_3$DEASbpy: ^{1}H NMR (200.13 MHz, CDCl$_3$): $\delta = 22.40$ (s, 2H, H-B), 15.95 (s, 3H, H-c), 12.30 (s, 2H, H-B), 11.56 (d, $J = 15.9$ Hz, 2H, H-7), 11.16 (d, $J = 15.9$ Hz, 2H, H-8), 9.40 (d, $J = 8.9$ Hz, 4H, H-10), 7.71 (d, $J = 8.9$ Hz, 4H, H-11), 6.93 (d, $J = 4.7$ Hz, 3H, H-T), 5.89 (s, 3H, H-T), 4.02 (q, $J = 6.9$ Hz, 8H, H-14), 3.74 (s, 3H, H-T), 1.68 (t, $J = 6.9$ Hz, 12H, H-15), -8.60 ppm (s, 3H, H-B). IR (KBr): $\tilde{\nu} = 1606$, 1589 cm^{-1} (vs. $\nu_{C=O}$). ^{19}F NMR (188.29 MHz, CDCl$_3$): $\delta = -86.97$ ppm. Elemental analysis calcd (%) for $C_{58}H_{50}F_9N_4O_6S_3Yb$: C 52.02, H 3.76, N 4.18; found: C 51.62, H 3.76, N 4.41.

[1] a) C. Andraud, O. Maury, *Eur. J. Inorg. Chem.* **2009**, 4357; b) Y. Ma, Y. Wang, *Coord. Chem. Rev.* **2010**, *254*, 972.

[2] a) C. P. Montgomery, B. S. Murray, E. J. New, R. Pal, D. Parker, *Acc. Chem. Res.* **2009**, *42*, 925; b) E. G. Moore, A. P. S. Samuel, K. N. Raymond, *Acc. Chem. Res.* **2009**, *42*, 542; c) S. V. Eliseeva, J.-C. G. Bünzli, *Chem. Soc. Rev.* **2010**, *39*, 189; d) J.-C. G. Bünzli, S. V. Eliseeva *Lanthanide Luminescence – Photophysical, Analytical and Biological Aspects in Springer Series on Fluorescence Vol. 7* (Eds.: P. Hännen, H. Härmä), Springer, Berlin, **2010**, ch. 1.

[3] G. S. He, L.-S. Tan, Q. Zheng, P. N. Prasad, *Chem. Rev.* **2008**, *108*, 1245.

[4] G. Piszczek, B. P. Maliwal, I. Gryczynski, J. Dattelbaum, J. R. Lakowicz, *J. Fluoresc.* **2001**, *11*, 101.

[5] a) M. H. V. Werts, N. Nerambourg, D. Pélégry, Y. Le Grand, M. Blanchard-Desce, *Photochem. Photobiol. Sci.* **2005**, *4*, 531; b) L.-M. Fu, X.-F. Wen, X.-C. Ai, Y. Sun, Y.-S. Wu, J.-P. Zhang, Y. Wang, *Angew. Chem.* **2005**, *117*, 757; *Angew. Chem. Int. Ed.* **2005**, *44*, 747; c) A. D'Aléo, A. Picot, P. L. Baldeck, C. Andraud, O. Maury, *Inorg. Chem.* **2008**, *47*, 10269.

[6] a) A. D'Aléo, G. Pompidor, B. Elena, J. Vicat, P. L. Baldeck, L. Toupet, R. Kahn, C. Andraud, O. Maury, *ChemPhysChem* **2007**, *8*, 2125; b) G.-L. Law, K.-L. Wong, C. W.-Y. Man, W.-T. Wong, S.-W. Tsao, M. H.-W. Lam, P. K.-S. Lam, *J. Am. Chem. Soc.* **2008**, *130*, 3714; c) F. Kielar, A. Congreve, G.-l. Law, E. J. New, D. Parker, K.-L. Wong, P. Castreno, J. de Mendoza, *Chem. Commun.* **2008**, 2435; d) F. Kielar, G.-L. Law, E. J. New, D. Parker, *Org. Biomol. Chem.* **2008**, *6*, 2256.

[7] a) A. Picot, A. D'Aléo, P. L. Baldeck, A. Grichine, A. Duperray, C. Andraud, O. Maury, *J. Am. Chem. Soc.* **2008**, *130*, 1532; b) S. V. Eliseeva, G. Auböck, F. van Mourik, A. Cannizzo, B. Song, E. Deiters, A.-S. Chauvin, M. Chergui, J.-C. G. Bünzli, *J. Phys. Chem. B* **2010**, *114*, 2932; c) Z.-J. Hu, X.-H. Tian, X.-H. Zhao, P. Wang, Q. Zhang, P.-P. Sun, J.-Y. Wu, J.-X. Yang, Y.-P. Tian, *Chem. Commun.* **2011**, *47*, 12467; d) W.-S. Lo, W.-M. Kwok, G.-L. Law, C.-T. Yeung, C. T.-L. Chan, H.-L. Yeung, H.-K. Kong, C.-H. Chen, M. B. Murphy, K.-L. Wong, W.-T. Wong, *Inorg. Chem.* **2011**, *50*, 5309.

[8] a) G. Piszczek, I. Gryczynski, B. P. Maliwal, J. R. Lakowicz, *J. Fluoresc.* **2002**, *12*, 15; b) T. Zhang, X. Zhu, C. C. W. Cheng, W.-M. Kwok, H.-L. Tam, J. Hao, D. W. J. Kwong, W.-K. Wong, K.-L. Wong, *J. Am. Chem. Soc.* **2011**, *133*, 20120; c) T. Zhang, X. Zhu, W.-K. Wong, H.-L. Tam, W.-Y. Wong, *Chem. Eur. J.* **2013**, *19*, 739.

[9] A. D'Aléo, A. Bourdolle, S. Brustlein, T. Fauquier, A. Grichine, A. Duperray, P. L. Baldeck, C. Andraud, S. Brasselet, O. Maury, *Angew. Chem.* **2012**, *124*, 6726; *Angew. Chem. Int. Ed.* **2012**, *51*, 6622.

[10] a) A. Hilton, T. Renouard, O. Maury, H. Le Bozec, I. Ledoux, J. Zyss, *Chem. Commun.* **1999**, 2521; b) A. Baccouche, B. Peigne, F. Ibersiene, D. Hammoutene, A. Boutarfaïa, A. Boucekkine, C. Feuvrie, O. Maury, I. Ledoux, H. Le Bozec, *J. Phys. Chem. A* **2010**, *114*, 5429.

[11] a) C. Feuvrie, O. Maury, H. Le Bozec, I. Ledoux, J. P. Morrall, G. T. Dalton, M. Samoc, M. G. Humphrey, *J. Phys. Chem. A* **2007**, *111*, 8980; b) C. Dragonetti, M. Balordi, A. Colombo, D. Roberto, R. Ugo, I. Fortunati, E. Garbin, C. Ferrante, R. Bozio, A. Abbotto, H. Le Bozec, *Chem. Phys. Lett.* **2009**, *475*, 245; c) N. Rendón, A. Bourdolle, P. L. Baldeck, H. Le Bozec, C. Andraud, S. Brasselet, C. Copéret, O. Maury, *Chem. Mater.* **2011**, *23*, 3228.

[12] See, for example: a) C. R. De Silva, J. R. Maeyer, R. Wang, G. S. Nichol, Z. Zheng, *Inorg. Chim. Acta* **2007**, *360*, 3543; b) G. Zucchi, V. Murugesan, D. Tondelier, D. Aldakov, T. Jeon, F. Yang, P. Thuéry, M. Ephritikhine, B. Geffroy, *Inorg. Chem.* **2011**, *50*, 4851.

[13] a) C. Freund, W. Porzio, U. Giovanella, F. Vignali, M. Pasini, S. Destri, A. Mech, S. Di Pietro, L. Di Bari, P. Mineo, *Inorg. Chem.* **2011**, *50*, 5417; b) A. Zaim, H. Nozary, L. Guénée, C. Besnard, J.-F. Lemmonier, S. Petoud, C. Piguet, *Chem. Eur. J.* **2012**, *18*, 7155.

[14] a) B. Wang, M. R. Wasielewski, *J. Am. Chem. Soc.* **1997**, *119*, 12; b) K. Sénéchal, L. Toupet, I. Ledoux, J. Zyss, H. Le Bozec, O. Maury, *Chem. Commun.* **2004**, 2180.

[15] a) A. D'Aléo, L. Ouahab, C. Andraud, F. Pointillart, O. Maury, *Coord. Chem. Rev.* **2012**, *256*, 1604; b) A. D'Aléo, A. Picot, A. Beeby, J. A. G. Williams, B. Le Guennic, C. Andraud, O. Maury, *Inorg. Chem.* **2008**, *47*, 10258; c) C. Yang, L.-M. Fu, Y. Wang, J.-P. Zhang, W.-T. Wong, X.-C. Ai, Y.-F. Qiao, B.-S. Zou, L.-L. Gui, *Angew. Chem.* **2004**, *116*, 5120; *Angew. Chem. Int. Ed.* **2004**, *43*, 5010.

[16] a) N. M. Shavaleev, S. J. A. Pope, Z. R. Bell, S. Faulkner, M. D. Ward, *Dalton Trans.* **2003**, 808; b) E. Di Piazza, L. Norel, K. Costuas, A. Bourdolle, O. Maury, S. Rigaut, *J. Am. Chem. Soc.* **2011**, *133*, 6174.

[17] a) N. Tancrez, C. Feuvrie, I. Ledoux, J. Zyss, L. Toupet, H. Le Bozec, O. Maury, *J. Am. Chem. Soc.* **2005**, *127*, 13474; b) K. Sénéchal-David, A. Hemeryck, N. Tancrez, L. Toupet, J. A. G. Williams, I. Ledoux, J. Zyss, A. Boucekkine, J.-P. Guégan, H. Le Bozec, O. Maury, *J. Am. Chem. Soc.* **2006**, *128*, 12243; c) G. L. Law, K. L. Wong, K. K. Lau, S. T. Lap, P. A. Tanner, F. Kuo, W. T. Wong, *J. Mater. Chem.* **2010**, *20*, 4074; d) A. Valore, E. Cariati, S. Righetto, D. Roberto, F. Tessore, R. Ugo, I. L. Fragala, M. E. Fragala, G. Malandrino, F. De Angelis, L. Belpassi, I. Ledoux-Rak, K. H. Thi, J. Zyss, *J. Am. Chem. Soc.* **2010**, *132*, 4966; e) J. W. Walton, R. Carr, N. H. Evans, A. M. Funk, A. M. Kenwright, D. Parker, D. S. Yufit, M. Botta, S. De Pinto, K. L. Wong, *Inorg. Chem.* **2012**, *51*, 8042.

[18] a) I. M. Batyaev, S. M. Shilov, M. Kolani, *Zh. Prikl. Spektrosk.* **1992**, *57*, 484; b) I. M. Batyaev, *J. Appl. Spectrosc.* **1997**, *64*, 620.

[19] O. Maury, J.-P. Guégan, T. Renouard, A. Hilton, P. Dupau, N. Sandon, L. Toupet, H. Le Bozec, *New J. Chem.* **2001**, *25*, 1553.

[20] C. Xu, W. W. Webb, *J. Opt. Soc. Am. B* **1996**, *13*, 481.

[21] M. Sheik-Bahae, A. A. Said, T. H. Wei, D. J. Hagan, E. W. Van Stryland, *IEEE J. Quantum Electron.* **1990**, *26*, 760.

[22] K. Kamada, K. Matsunaga, A. Yoshino, K. Ohta, *J. Opt. Soc. Am. B* **2003**, *20*, 529.

[23] K. Kamada, Y. Iwase, K. Sakai, K. Kondo, K. Ohta, *J. Phys. Chem. C* **2009**, *113*, 11469.